



# Behavior of the central intensity of generalized humbert-gaussian beams against the atmospheric turbulence

N. Nossir<sup>1</sup> · L. Dalil-Essakali<sup>1</sup> · A. Belafhal<sup>1</sup>

Received: 1 May 2021 / Accepted: 16 October 2021 / Published online: 2 November 2021

© The Author(s), under exclusive licence to Springer Science+Business Media, LLC, part of Springer Nature 2021

## Abstract

In this paper, we present a theoretical study of the propagation properties for Generalized Humbert-Gaussian beams (GHGBs) passing through a turbulent atmosphere. The axial intensity distribution of beams propagating through atmospheric turbulence is evaluated analytically based on the Huygens-Fresnel diffraction integral and the Rytov theory. The impact of the incident beam parameters and the turbulent strength on the output axial intensity is investigated through numerical illustrations. The results show that the propagation of GHGBs is faster when the atmosphere is very turbulent for small wavelength and small beam waist.

**Keywords** Generalized Humbert-Gaussian beams · Turbulent atmosphere · Huygens-Fresnel diffraction integral · Rytov theory

## 1 Introduction

The propagation of laser beams in a turbulent atmosphere has received a lot of attention from many researchers for several years, due to their large applications in many areas of science and practical engineering including free space optical communications (Navidpour et al. 2007), active optical imaging system (Hajjarian et al. 2010), and remote sensing (Korotkova and Gbur 2007). On the other hand, the turbulent atmosphere has an important impact on the quality of the laser beam owing to the random changes in the refraction index along the path of beam propagation. This result from the small temperature variations in the atmosphere, which induce fluctuations in laser intensity.

In the literature, several works have focused on the study of the influence of the turbulent atmospheric environment on the propagation of laser beams (Eyyuboğlu 2008; Wang and Zheng 2009; Qing et al. 2014; Mei et al. 2012; Zhou et al. 2009; Wen et al. 2015). The propagation properties of elegant Laguerre-Gaussian beams (Qu et al. 2010), Laguerre-Gaussian Beams (Banakh and Falits 2014), flat-topped vortex hollow

---

✉ A. Belafhal  
belafhal@gmail.com

<sup>1</sup> Laboratory LPNAMME, Laser Physics Group, Department of Physics, Faculty of Sciences, Chouaib Doukkali University, P. B 20, El Jadida 24000, Morocco

beams (Liu et al. 2016), Laguerre-Gaussian Schell beams (Xu et al. 2014), truncated Bessel-Gauss beams (Cang and Zhang 2010), partially coherent Bessel-Gaussian beams (Chen et al. 2008) and Hypergeometric-Gaussian beams (Tanyer Eyyuboglu and Cai 2012) and so on, have greatly developed by the considered authors. On the other hand, in our research group Khannous et al. have interested to the propagation characteristics of some laser beams in turbulent atmosphere such as: Kummer beams (Khannous et al. 2014), Hypergeometric-Gaussian beams Type II (Khannous et al. 2015) and Hollow-Gaussian beams (Khannous et al. 2016). Hennani et al. (Hennani et al. 2013) have studied the axial intensity distribution of the modified quadratic Bessel-Gaussian beam in turbulent atmosphere. Kinani et al. (Kinani et al. 2011) have examined the effects of the atmospheric turbulence on the propagating of Li's flat-topped beams. More recently, Ez-zariy et al. (Ez-zariy et al. 2016) have investigated the propagation of Lommel-Gaussian beams through atmospheric turbulence, Boufalah et al. (Boufalah et al. 2016, 2018) have reported a study of the propagation of Pearcey-Gaussian beam and Generalized Laguerre-Bessel-Gaussian beams in turbulent atmosphere and Yaalou et al. (Yaalou et al. 2019; Hricha et al. 2020) have developed theoretically the propagation characteristics of dark and antidark-Gaussian beams and double-half inverse Gaussian hollow beams in turbulent atmosphere.

We will interest in the present study to the propagation properties of the Generalized Humbert beams modulated by Gaussian envelope (GHGBs) in turbulent atmosphere, where the Generalized Humbert beams (GHBs) are new hollow beams generated recently by Belafhal and Saad (Belafhal and Nebdi 2014). These last beams can be created by illuminating Circular beams (CiBs) (M. A. Bandres J. C. Gutierrez-Vega 2008) with a spiral phase plate (SPP) passing through a paraxial ABCD optical system. The particular cases of GHGBs presented in this work are generated from Whittaker-Gaussian beams (WGBs), Hypergeometric-Gaussian beams (HyGBs), elegant Laguerre-Gaussian beams (eLGBs), standard Gaussian Laguerre beams (sLGBs), Generalized Laguerre-Gaussian beams (gLGBs) or quadratic Bessel-Gaussian beams (QBGBs) by the manipulation of the input beam parameters. This family of beams will give rise to different particular cases beams of GHGBs and possesses interesting properties; which are advantages for certain applications. For this reason, our attention was concentrated to study the behavior of this beams family during its propagation in a turbulent atmosphere.

The coming parts of this article are structured as follows: Sect. 2 is devoted to perform the average intensity distribution of GHGBs propagating in atmospheric turbulence. An approximate analytical expression of the axial intensity distribution for the considered beams is expressed in Sect. 3. In Sect. 4, special cases of GHGBs are derived. The numerical simulations and discussions are treated in Sect. 5. A conclusion is outlined in the end of this work.

## 2 The average intensity distribution of GHGBs in a turbulent atmosphere

Let us consider the electric field distribution of GHGBs in the cylindrical coordinates system  $(r, z_0, \phi)$  given by Belafhal and Nebdi (2014)

$$E_{GHBS}(r, z_0, \theta) = A_l^m r^{m+l} \exp\left(\frac{ik}{2z_0} r^2\right) \exp[i(m+l)\theta] \times \Psi_1\left(m + \frac{l}{2} + 1, \beta; m+l+1; m+1; \frac{2i\alpha'}{\alpha+i\alpha'}, \frac{-(k/z_0)^2}{4(\alpha+i\alpha')} r^2\right), \tag{1}$$

where

$$A_l^m = -E_f \frac{\Gamma(\frac{l}{2} + m + 1)}{\Gamma(m+l+1)} \left(\frac{ik}{z_0}\right)^{m+l+1} \left(\frac{1}{\alpha+i\alpha'}\right)^{\frac{l}{2}+m+1} \frac{(i\alpha')^{\frac{m}{2}}}{2^{\frac{m}{2}+l+1}} \exp[ik(z_0+z')] \frac{(1+z'/\tilde{q}_0)^{(m+1)/2-\beta}}{(1+z'/q_0)^{(m+3)/2-\beta}}, \tag{2a}$$

with

$$\alpha = -ik \left[ \frac{\omega_0^2}{4} \left( \frac{1}{z'+\tilde{q}_0} + \frac{1}{z'+q_0} \right) + \frac{1}{2z_0} \right], \tag{2b}$$

$$\alpha' = \frac{\omega_0^2}{4k \left( \frac{1}{z'+q_0} + \frac{1}{z'+q_0} \right)}, \tag{2c}$$

and

$$\beta = \frac{m+1-\mu}{2}, \tag{2d}$$

$E_f$  is the amplitude of the beam,  $\omega_0$  is the spot size of the fundamental Gaussian mode,  $\mu$  is the radial order,  $(q_0, \tilde{q}_0)$  are two complex beam parameters,  $k = \frac{2\pi}{\lambda}$  represents the wave number,  $\lambda$  is the wavelength,  $l$  is the topological charge,  $m$  is the beam order,  $\Gamma(\cdot)$  denotes the gamma function and  $\Psi_1(\cdot)$  is the Humbert confluent hypergeometric function. We consider that the field is situated at a distance  $z = z_0$  from the source plane, with  $z'$  is the transverse coordinate of the Circular beams.

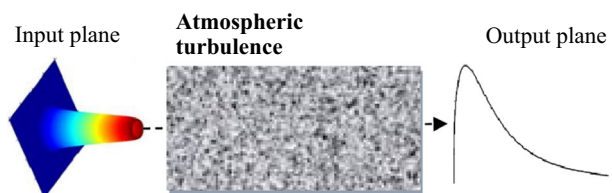
In the following, we will interest to the Generalized Humbert beams modulated by a Gaussian envelope. The electric field expression of these beams is given by Nossir et al. 2020a; Nossir et al. 2020b)

$$E_{GHGBs}(r, z_0, \theta) = E_{GHBS}(r, z_0, \theta) \exp\left(\frac{-nr^2}{\omega_0^2}\right), \tag{3}$$

with  $\eta$  is a positive constant.

The optical system representing the propagation of the GHGBs through a turbulent atmosphere is schematized in Fig. 1. The receiver plane is positioned at propagation distance  $z$  away from the transmitter plane.

**Fig. 1** Schematic illustration of the GHGBs propagating in a turbulent atmosphere



In this section, we will interest to the determination of the analytical average intensity distribution of GHGBs propagating in the turbulent atmosphere.

Based on the extended Huygens-Fresnel diffraction integral in the paraxial approximation and on the Rytov theory, the average intensity at the output plane is expressed as (Andrews and Phillips 1998)

$$E(\vec{\rho}, z, t) = \frac{-ik}{2\pi z} \exp(ikz) \int_0^a \int_0^{2\pi} E(\vec{r}, z_0) \exp \left[ \frac{ik}{2z} (\vec{r} - \vec{\rho}) + \Phi(\vec{r}, \vec{\rho}) - 2i\pi \cdot f \cdot t \right] d\vec{r}, \tag{4}$$

where  $z$  is the propagation distance,  $a$  is the radius of the aperture,  $\Phi(\vec{r}, \vec{\rho})$  represents the random part, in the Rytov method, of the complex phase of a spherical wave propagating from the source plane to the output plane,  $f$  is the frequency and  $t$  denotes the time. Here  $E(\vec{r}, z_0)$  is the electric field of the GHGBs at the input plane.

The average intensity distribution at the  $z$ -plane can be written as

$$\begin{aligned} \langle I(\vec{\rho}, z) \rangle &= \langle E(\vec{\rho}, z, t) \rangle \langle E^*(\vec{\rho}, z, t) \rangle \\ &= \frac{k^2}{4\pi^2 z^2} \int_0^a \int_0^a \int_0^{2\pi} \int_0^{2\pi} E(\vec{r}_1, z_0) \cdot E^*(\vec{r}_2, z_0) \exp \left[ \frac{ik}{2z} (\vec{r}_1 - \vec{\rho})^2 - \frac{ik}{2z} (\vec{r}_2 - \vec{\rho})^2 \right] \\ &\quad \times \langle \exp [\Phi(r_1, \vec{\rho}) + \langle \Phi^*(r_2, \vec{\rho}) \rangle] \rangle d\vec{r}_1 d\vec{r}_2, \end{aligned} \tag{5}$$

where the average term in the last equation is given by Andrews and Phillips (1998)

$$\langle \exp \{ \Phi(r_1, \rho) + \langle \Phi^*(r_2, \vec{\rho}) \rangle \} \rangle = \exp [-0.5D_\Phi(\vec{r}_1 - \vec{r}_2)] \tag{6a}$$

In these equations, asterisk  $*$  denotes the complex conjugate,  $\langle \rangle$  is the average,  $D_\Phi(\vec{r}_1 - \vec{r}_2)$  is the phase structure function of the random complex in Rytov's representation given by

$$D_\Phi(\vec{r}_1 - \vec{r}_2) = \frac{2}{\rho_0} (\vec{r}_1 - \vec{r}_2)^2 \tag{6b}$$

with

$$\rho_0 = (0.545C_n^2 K^2 z)^{-3/5} \tag{6c}$$

is the coherence length of a spherical wave spreading in the turbulent atmosphere medium where  $C_n^2$  is the refractive index structure constant, which characterizes the local strength of the turbulent atmosphere. By using the development of Humbert confluent hypergeometric function in terms of the Hypergeometric function  ${}_2F_1(a, b; c; x)$  (Luke 1969)

$$\psi_1(a, b; c; c'; w, z) = \sum_{n=0}^{\infty} \frac{(a)_n z^n}{(c')_n n!^2} F_1(a + n; b; c; w) \tag{7}$$

and by introducing Eqs. (3), (6a), (6b) and (7) into Eq. (5), we can evaluate the average intensity distribution of GHGBs as

$$\begin{aligned}
 \langle I(\vec{\rho}, z) \rangle &= \frac{A_L^m A_L^{m*}}{\lambda^2 z^2} \sum_{q=0}^{\infty} \frac{\Gamma(\frac{l}{2} + m + 1 + q)}{q! \Gamma(m + 1 + q)} \left( \frac{-(k/z_0)^2}{4(\alpha + i\alpha')} \right)^q \sum_{j=0}^{\infty} \frac{\Gamma(\frac{l}{2} + m + 1 + j)}{j! \Gamma(m + 1 + j)} \left( \frac{-(k/z_0)^2}{4(\alpha + i\alpha')^*} \right)^j \\
 &\times {}_2F_1\left(\frac{l}{2} + m + 1 + q, \beta; m + l + 1; \frac{2i\alpha'}{\alpha + i\alpha'}\right) {}_2F_1\left(\frac{l}{2} + m + 1 + j, \beta; m + l + 1; \left(\frac{2i\alpha'}{\alpha + i\alpha'}\right)^*\right) \\
 &\times \int_0^a \int_0^a \int_0^{2\pi} \int_0^{2\pi} r_1^{m+l+2q+1} r_2^{m+l+2j+1} \exp[i(m+l)(\theta_1 - \theta_2)] \exp\left[\frac{2 \cos(\theta_1 - \theta_2) r_1 r_2}{\rho_0^2}\right] \\
 &\times \exp\left[-\left\{\frac{ik}{2}\left(\frac{1}{z} + \frac{1}{z_0}\right) + \left(\frac{\eta}{\omega_0^2} + \frac{1}{\rho_0^2}\right)\right\} r_2^2\right] \exp\left[\left\{\frac{ik}{2}\left(\frac{1}{z} + \frac{1}{z_0}\right) - \left(\frac{\eta}{\omega_0^2} + \frac{1}{\rho_0^2}\right)\right\} r_1^2\right] \\
 &\times \exp\left[\frac{ik}{2z} \rho(r_1 \cos(\theta_1 - \varphi) - r_2 \cos(\theta_2 - \varphi))\right] dr_1 dr_2 d\theta_1 d\theta_2.
 \end{aligned} \tag{8}$$

From Eq. (8), we will deduce the on-axis average intensity distribution of GHGBs propagating in turbulent atmosphere in the following section.

### 3 Axial intensity distribution of truncated GHGBs in turbulent atmosphere

In this part, we will give an approximate evaluation of the axial intensity distribution of the GHGBs propagating in a turbulent atmosphere. To evaluate the integral of Eq. (8), we will introduce the hard aperture function defined as

$$H(r) = \begin{cases} 1 & |r| \leq a \\ 0 & |r| > a \end{cases} \tag{9}$$

with  $a$  is the half-width of the rectangular function.

The approximate expression of  $H(r)$  is given by expanding into a finite sum of complex Gaussian functions with finite numbers in the rectangular coordinates system (Wen et al. 1988)

$$H(r) = \sum_{k=1}^N A_k \exp\left[-\frac{B_k}{a^2} r^2\right] \tag{10}$$

where  $A_k$  and  $B_k$  designate the expansion and Gaussian coefficients, respectively.  $N$  is the number of the expansion of Gaussian function. By substituting Eq. (10) into Eq. (8) then, we put  $\rho = 0$  and the average axial intensity distribution becomes

$$\begin{aligned}
 \langle I(0, z) \rangle &= \frac{A_l^m A_l^{m*}}{\lambda^2 z^2} \sum_{q=0}^{\infty} \frac{\Gamma\left(\frac{l}{2} + m + 1 + q\right)}{q! \Gamma(m + 1 + q)} \left( \frac{-(k/z_0)^2}{4(\alpha + i\alpha')} \right)^q \\
 &\times {}_2F_1\left(\frac{l}{2} + m + 1 + q, \beta; m + l + 1; \frac{2i\alpha'}{\alpha + i\alpha'}\right) \sum_{j=0}^{\infty} \frac{\Gamma\left(\frac{l}{2} + m + 1 + j\right)}{j! \Gamma(m + 1 + j)} \left( \frac{-(k/z_0)^2}{4(\alpha + i\alpha')} \right)^j \\
 &\times {}_2F_1\left(\frac{l}{2} + m + 1 + j, \beta; m + l + 1; \frac{2i\alpha'}{\alpha + i\alpha'}\right) \sum_{g=1}^N A_g \sum_{s=1}^N A_s \\
 &\int_0^{+\infty} \int_0^{+\infty} \int_0^{2\pi} \int_0^{2\pi} \exp\left(\frac{2r_1 r_2}{\rho_0^2} \cos(\theta_2 - \theta_1)\right) \exp(-r_1^2 \beta_1) \exp(-r_2^2 \beta_2) \exp(-i(m+1)\theta_2) \\
 &\times \exp(i(m+l)\theta_1) r_1^{m+l+2j+1} r_2^{m+l+2q+1} dr_1 dr_2 d\theta_1 d\theta_2,
 \end{aligned} \tag{11}$$

with

$$\beta_1 = \left( \frac{\eta}{\omega_0^2} + \frac{1}{\rho_0^2} + \frac{B_g}{a^2} \right) - \frac{ik}{2} \left( \frac{1}{z_0} + \frac{1}{z} \right) \tag{12a}$$

and

$$\beta_2 = \left( \frac{\eta}{\omega_0^2} + \frac{1}{\rho_0^2} + \frac{B_g}{a^2} + \frac{ik}{2} \left( \frac{1}{z_0} + \frac{1}{z} \right) \right) \tag{12b}$$

For resolution of the integrals in Eq. (11), we will apply the well-known formulas (Gradshteyn and Ryzhik 1994)

$$\int_0^{2\pi} \exp(-im\varphi_2 + x \cos(\varphi_2 - \varphi_1)) d\varphi_2 = 2\pi \exp(-im\varphi_1) I_m(x), \tag{13}$$

and

$$\begin{aligned}
 &\int_0^{+\infty} x^{\delta'-1} \exp(-\mu'x) {}_mF_n(\alpha_1, \alpha_2, \dots, \alpha_m; \gamma_1, \gamma_2, \dots, \gamma_m; \lambda x) dx = \Gamma(\delta') \mu'^{-\delta'} \\
 &\times {}_{m+1}F_n\left(\alpha_1, \alpha_2, \dots, \alpha_m; \gamma_1, \gamma_2, \dots, \gamma_m; \frac{\lambda}{\mu'}\right) [m \leq n, \text{Re } \delta' > 0; \text{Re } \mu' > 0, \text{ if } m < n; \text{Re } \mu' > \lambda, \text{ if } m = n],
 \end{aligned} \tag{14}$$

where  $I_m(\cdot)$  is the m-order modified Bessel function and  ${}_mF_n$  is the confluent Hypergeometric function. After some algebraic calculations, we find the analytical expression of the axial intensity distribution of GHGBs as follows

$$\begin{aligned}
 \langle I(z, 0) \rangle &= \frac{k^2}{4z^2} \frac{A_l^m A_l^{m*}}{\rho_0^{2m+2l}} \left[ \frac{\Gamma\left(\frac{l}{2} + m + 1\right)}{m!} \right]^2 \Gamma(m + l + 1) \sum_{g=1}^N A_g \sum_{s=1}^N A_s \left(\frac{1}{\beta_1 \beta_2}\right)^{m+l+1} \\
 &\times \sum_{q=0}^{\infty} \frac{\left(\frac{l}{2} + m + 1\right)_q (m + l + 1)_q}{(m + 1)_q} \frac{\left(\frac{-(k/z_0)^2}{4(\alpha + i\alpha')\beta_1}\right)^q}{q!} {}_2F_1\left(\frac{l}{2} + m + 1 + q, \beta; m + l + 1; \frac{2i\alpha'}{\alpha + i\alpha'}\right) \\
 &\times \sum_{j=0}^{\infty} \frac{\left(\frac{l}{2} + m + 1\right)_j (m + l + 1)_j}{(m + 1)_j} \frac{\left(\frac{-(k/z_0)^2}{4(\alpha + i\alpha')^* \beta_2}\right)^j}{j!} {}_2F_1\left(\frac{l}{2} + m + 1 + j, \beta; m + l + 1; \left(\frac{2i\alpha'}{\alpha + i\alpha'}\right)^*\right) \\
 &\times {}_2F_1\left(m + l + 1 + j, m + l + 1 + q; m + l + 1; \frac{1}{\beta_2 \beta_1 \rho_0^4}\right),
 \end{aligned} \tag{15}$$

This last equation is the main result obtained in this work. To understand the GHGBs properties propagating in atmospheric turbulence, we will treat, in the next section, some particular cases by using Eq. (15).

### 4 Particular cases of GHGBs

We note that from Eq. (15) we can obtain the particular cases of GHGBs denoted by  $GHGBs_{QBGBs}$ ,  $GHGBs_{WGBs}$ ,  $GHGBs_{sLGBs}$ ,  $GHGBs_{eLGBs}$ ,  $GHGBs_{gLGBs}$  and  $GHGBs_{HyGGBs}$  and given in Table 1. Here,  $n$  is the high radial order of  $eLGBs$  and  $sLGBs$  beams,  $l$  is the beam parameter of the CiBs and  $h$  is a positive real number. In Table 1,  $d_1^+$ ,  $d_1^-$ ,  $d_2^+$ ,  $d_2^-$ ,  $d_3^+$  and  $d_3^-$  are defined as

$$d_1^+ = \frac{2(h + i)}{2z'(h + i) + k\omega_0^2}, \tag{16a}$$

**Table 1** Parameters of particular beams

Beams	Parameters of input beams			Parameters of output beams	
$GHGBs$	$\frac{m+1-\mu}{2}$	$q_0$	$\tilde{q}_0$	$\alpha$	$\alpha'$
$GHGBs_{sLGBs}$	$-n$	$q_0$	$\tilde{q}_0^*$	$-ik\left(\frac{\omega_0^2}{4}d_2^+ + \frac{1}{2z_0}\right)$	$\frac{k\omega_0^2}{4}d_2^-$
$GHGBs_{eLGBs}$	$-n$	$q_0$	$\infty$	$-ik\left(\frac{\omega_0^2}{4}d_2^+ + \frac{1}{2z_0}\right)$	$-ik\left(\frac{\omega_0^2}{4}d_2^+ + \frac{1}{2z_0}\right)$
$GHGBs_{QBGBs}$	$\frac{m+1}{2}$	$-\tilde{q}_0^*$	$\frac{k\omega_0^2}{2(h+i)}$	$-ik\left[\frac{\omega_0^2}{4}(d_1^+ + d_2^-) + \frac{1}{2z_0}\right]$	$\frac{k\omega_0^2}{4}(d_1^- - d_2^+)$
$GHGBs_{WGBs}$	$\frac{m+1-\mu}{2}$	$\tilde{q}_0^*$	$\frac{k\omega_0^2}{2(h+i)}$	$-ik\left[\frac{\omega_0^2}{4}(d_1^+ + d_2^-) + \frac{1}{2z_0}\right]$	$\frac{k\omega_0^2}{4}(d_1^- - d_2^+)$
$GHGBs_{gLGBs}$	$-n$	$q_0$	$\tilde{q}_0$	$-ik\left(\frac{\omega_0^2}{4}d_3^+ + \frac{1}{2z_0}\right)$	$\frac{k\omega_0^2}{4}d_3^-$
$GHGBs_{HyGGBs}$	$\frac{-\mu}{2}$	$q_0$	$0$	$-ik\left[\frac{\omega_0^2}{4}\left(\frac{1}{z'} + \frac{1}{q_0+z'}\right) + \frac{1}{2z_0}\right]$	$\frac{k\omega_0^2}{4}\left[\frac{1}{z'} - \frac{1}{q_0+z'}\right]$

$$d_1^- = \frac{2(h-i)}{2z'(h-i) - k\omega_0^2}, \quad (16b)$$

$$d_2^+ = \frac{1}{q_0^* + z'} + \frac{1}{q_0 + z'}, \quad (16c)$$

$$d_2^- = \frac{1}{\tilde{q}_0^* + z'} + \frac{1}{q_0 + z'}, \quad (16d)$$

$$d_3^+ = \frac{1}{\tilde{q}_0 + z'} + \frac{1}{q_0 + z'}, \quad (16e)$$

and

$$d_3^- = \frac{1}{q_o + z'} - \frac{1}{q_o + z'}, \quad (16f)$$

## 5 Numerical examples and analysis

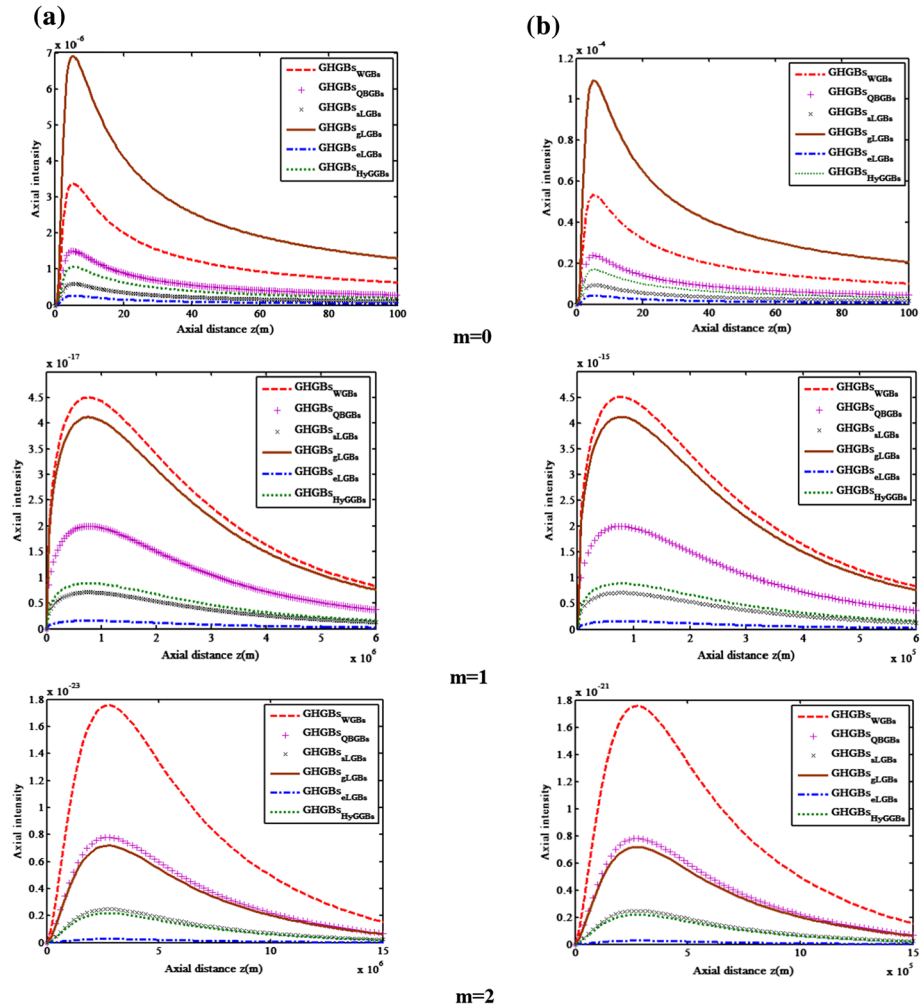
In this section, using the analytical expression of the average intensity distribution of GHGBs propagating in atmospheric turbulence derived in Sect. 3, we present some numerical results of the propagation characteristics for the particular cases of GHGBs given in Table 1.

Figure 2 shows the evolution of the distribution of the axial intensity for GHGBs versus the propagation distance  $z$ . The plots are given for three values of the beam orders:  $m = 0$ ,  $m = 1$ , and  $m = 2$  and for two values of the turbulent strengths  $C_n^2 = 1.10^{-14}m^{-2/3}$  and  $C_n^2 = 1.10^{-15}m^{-2/3}$ . We can note from the plots that the intensity of GHGBs increases upon propagation when the atmosphere is very turbulent and the beam orders are small. Furthermore, it observed that  $GHGBs_{WGBs}$  present a high intensity in comparison with other beams while  $GHGBs_{eLGBs}$  are characterized by a small intensity. It is seen that the position of the maximum intensity tends toward small values of the propagation distance when  $C_n^2$  is large which means that the propagation distance of GHGBs family becomes shorter when the atmosphere is very turbulent.

To show the influence of the wavelength on the propagation of GHGBs, the distribution of the axial intensity is depicted versus the axial distance  $z$  in Fig. 3 for different beam orders ( $m=0, 1$  and  $m=2$ ). Several curves are plotted for two wavelength value  $\lambda = 632.8mm$  and  $\lambda = 1330mm$  with a fixed value of the turbulent strength  $C_n^2 = 1.10^{-14}m^{-2/3}$ . It can be observed that the greater the beam orders and the wavelength, the lower the axial intensity of GHGBs becomes.

It is clear that  $GHGBs_{eLGBs}$  have a minimal intensity, whereas the maximum intensity appears for the  $GHGBs_{WGBs}$  for all beam orders. However, we can also note that the position of the maximum intensity tends to higher values of propagation distance with large values of wavelength. We conclude that the GHGBs with small wavelength have a faster propagation in turbulent atmosphere.





**Fig. 2** The average axial intensity distribution versus the propagation distance  $z$  for GHGBs for different beam orders:  $m=0$ ,  $m=1$  and  $m=2$ , with two values of turbulent strength: **a**  $C_n^2 = 1.10^{-15} m^{-2/3}$  and **b**  $C_n^2 = 1.10^{-14} m^{-2/3}$ . The others parameters are chosen as:  $l = 1$ ,  $\omega_0 = 0.5 \text{ mm}$ ,  $\lambda = 1330 \text{ nm}$ ,  $a = 0.5 \text{ m}$ ,  $\mu = 1$  and  $h = 1$

Figure 4 represents the variation of on-axis average intensity of GHGBs with propagation distance  $z$  for  $\lambda = 1330 \text{ nm}$  and  $C_n^2 = 1.10^{-14} m^{-2/3}$ , with three beams orders.

For every beam, and for a fixed beam order, the curves are plotted for two beams waist  $\omega_0 = 0.5 \text{ mm}$  and  $\omega_0 = 0.8 \text{ mm}$ . The plots of the figure show that the average intensity of GHGBs propagating through an atmospheric turbulence becomes lower for higher values of the beam orders. It is noted that the  $GHGBs_{WGBs}$  have a higher intensity however  $GHGBs_{eLGBs}$  have the lower intensity compared to the other beams. We can deduct from Fig. 4, that the propagation distance for all beams becomes shorter when the beam waist is smaller.

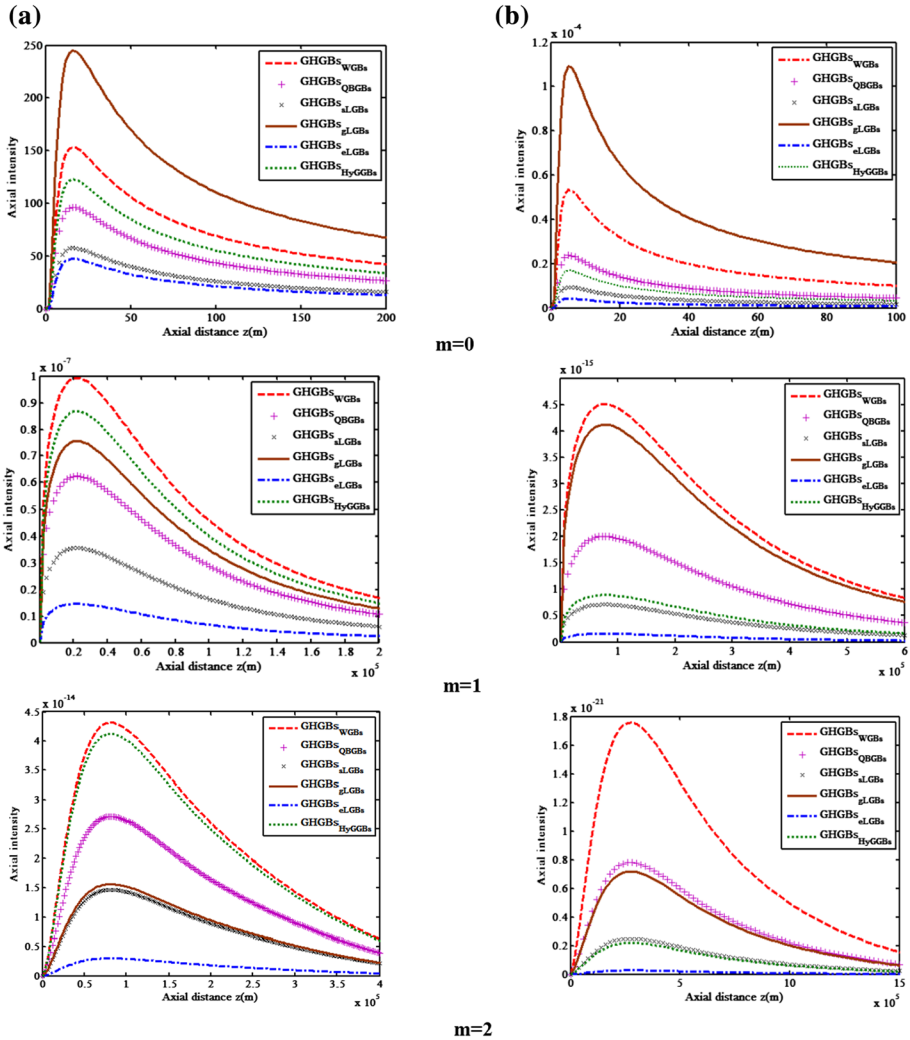


**Fig. 3** The average axial intensity distribution versus the propagation distance  $z$  for GHGBs for  $m=0$ ,  $m=1$ , and  $m=2$ , with different beam orders and two values of wavelength: **a**  $\lambda = 632.8 \text{ nm}$ , **b**  $\lambda = 1330 \text{ nm}$ . The other parameters are:  $\omega_0 = 0.5 \text{ mm}$ ,  $C_n^2 = 1.10 \cdot 10^{-14} \text{ m}^{-2/3}$ ,  $a = 0.5 \text{ m}$ ,  $\mu = 1$ ,  $h = 1$  and  $l = 1$

### 6 Conclusion

In this paper, we have discussed the propagation properties of GHGBs as hollow beams in a turbulent atmospheric environment. Through this study, we developed the average axial intensity distribution of GHGBs using the extended Huygens-Fresnel diffraction integral and the Rytov theory. We can conclude from the numerical results, that the propagation distance for GHGBs in turbulent atmosphere becomes shorter when the wavelength and the beam waist are small and the atmospheric environment is highly turbulent. The present study is a generalization of some special cases deduced from our

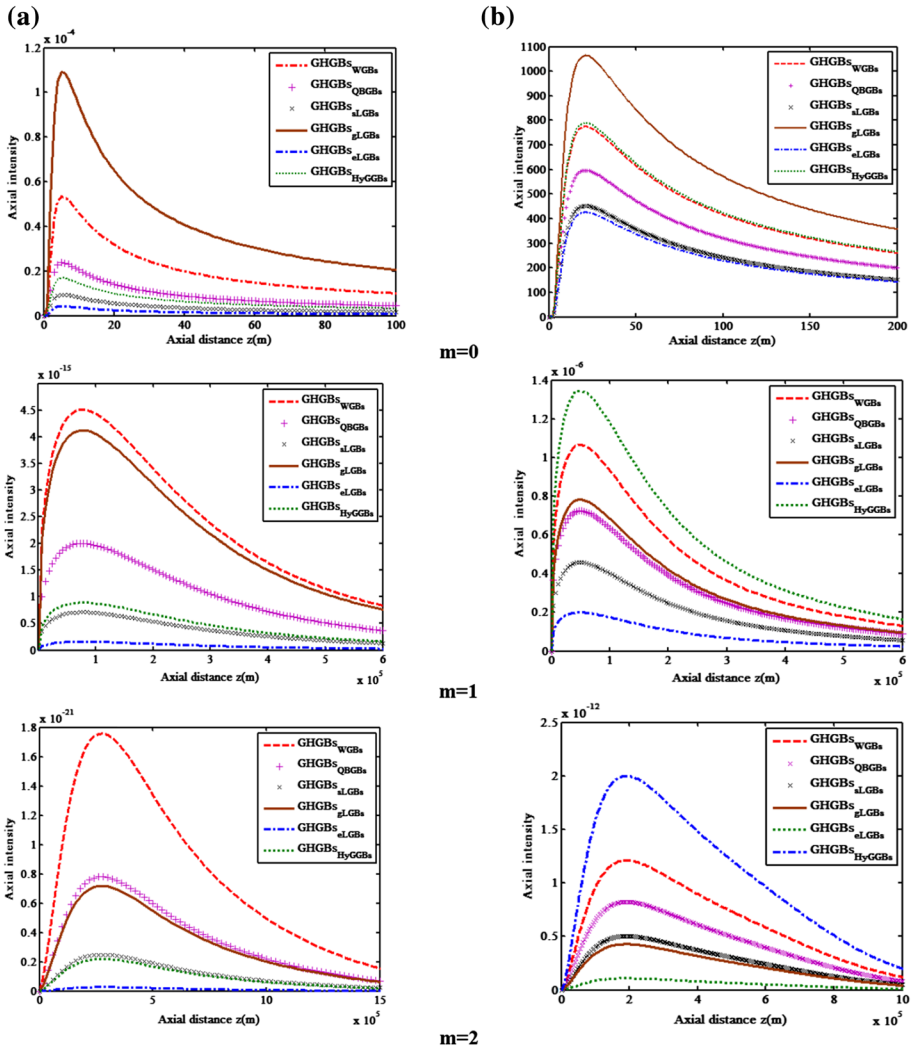


**Fig. 4** The average axial intensity distribution versus the propagation distance  $z$  for GHGBs with different beam orders:  $m=0$ ,  $m=1$ ,  $m=2$ , and for two values of the beams waist: **a**  $\omega_0 = 0.5\text{ mm}$  and **b**  $\omega_0 = 0.8\text{ mm}$ . The other parameters are:  $\lambda = 1330\text{ nm}$ ,  $C_n^2 = 1.10^{-14}\text{ m}^{-2/3}$ ,  $a = 0.5\text{ m}$ ,  $\mu = 1$ ,  $h = 1$  and  $l = 1$

finding result concerning the GHGBs. We can note that  $GHGBs_{WGBs}$  are characterized by the greatest intensity distribution in comparison with the other beams family during the propagation in turbulent atmosphere, which may be the more desirable for certain applications.

### References

Andrews, L., Phillips, R.: Laser beam propagation through random media. SPIE Press, Washington (1998)

- Banakh, V., Falits, A.V.: Turbulent broadening of Laguerre-Gaussian beam in the atmosphere. *Opt. Spectrosc.* **117**, 942–948 (2014)
- Bandres, M.A., Gutierrez-Vega, J.C.: Circular beams. *Opt. Lett.* **33**(2), 177–179 (2008)
- Belafhal, A., Nebdi, H.: Generation and propagation of novel donut beams by a spiral phase plate: Humbert beams. *Opt. Quantum Electron.* **46**, 201–208 (2014)
- Boufalah, F., Dalil-Essakali, L., Nebdi, H., Belafhal, A.: Effect of turbulent atmosphere on the on-axis average intensity of Pearcey-Gaussian beam. *Chin. Phys. b.* **25**, 064207–064213 (2016)
- Boufalah, F., Dalil-Essakali, L., Ez-zariy, L., Belafhal, A.: Introduction of generalized Bessel–Laguerre–Gaussian beams and its central intensity travelling a turbulent atmosphere. *Opt. Quantum Electron.* **50**, 3051–30520 (2018)
- Cang, J., Zhang, Y.: Axial intensity distribution of truncated Bessel-Gauss beams in a turbulent atmosphere. *Optik* **121**, 239–245 (2010)
- Chen, B., Chen, Z., Ji-Xiong, P.: Propagation of partially coherent Bessel-Gaussian beams in turbulent atmosphere. *Opt. Laser Technol.* **40**, 820–827 (2008)
- Eyyuboglu, H.T.: Propagation and coherence properties of higher order partially coherent dark hollow beams in turbulence. *Opt. Laser Technol.* **40**, 156–166 (2008)
- Ez-zariy, L., Boufalah, F., Dalil-Essakali, L., Belafhal, A.: Effects of a turbulent atmosphere on an apertured Lommel-Gaussian beam. *Optik* **127**, 11534–11543 (2016)
- Gradshteyn, I.S., Ryzhik, I.M.: *Tables of integrals, series and products*, 5th edn. Academic Press, New York (1994)
- Hajarian, Z., Kavehrad, M., Fadlullah, J.: Spatially multiplexed multi-input-multi-output optical imaging system in a turbid, turbulent atmosphere. *Appl. Opt.* **49**, 1528–1538 (2010)
- Hennani, S., Barmaki, S., Ez-zariy, L., Nebdi, H., Belafhal, A.: A theoretical investigation of the axial intensity distribution of truncated MQBG beam in a turbulent atmosphere. *Phys. Chem. News* **69**, 44–51 (2013)
- Hricha, Z., Yaalou, M., Belafhal, A.: Intensity characteristics of double-half inverse Gaussian hollow beams through turbulent atmosphere. *Opt. Quantum Electron.* **52**, 1–8 (2020)
- Khannous, F., Boustimi, M., Nebdi, H., Belafhal, A.: Propagation analysis of the superposition of Kummer beams in a turbulent atmosphere. *Phys. Chem. News* **73**, 83–89 (2014)
- Khannous, F., Boustimi, M., Nebdi, H., Belafhal, A.: On-axis average intensity of hypergeometric Gaussian beams type II propagating in a turbulent atmosphere. *J. Mater. Environ.* **6**, 2550–2556 (2015)
- Khannous, F., Boustimi, M., Nebdi, H., Belafhal, A.: Theoretical investigation on the Hollow Gaussian beams propagating in atmospheric turbulent. *Chin. J. Phys.* **54**(2), 194–204 (2016)
- Kinani, A., Ez-zariy, L., Chafiq, A., Nebdi, H., Belafhal, A.: Effects of atmospheric turbulence on the propagation of Li's flat-topped optical beams. *Phys. Chem. News* **61**, 24–33 (2011)
- Korotkova, O.A., Gbur, G.: Angular spectrum representation for propagation of random electromagnetic beams in a turbulent atmosphere. *J. Opt. Soc. Am. A Opt.* **24**, 2728–2736 (2007)
- Liu, D., Wang, Y., Wang, G., Yin, H.: Intensity properties of flat-topped vortex hollow beams propagating in atmospheric turbulence. *Optik* **20**, 9386–9393 (2016)
- Luke, Y.L.: *The special functions and their approximation*, vol. I. Academic Press, Cambridge (1969)
- Mei, Q.X., Yue, Z.W., Zhong, R.R.: Long-distance propagation of pseudo-partially coherent Gaussian Schell-model beams in atmospheric turbulence. *Chin. Phys. B.* **21**(9), 094202 (2012)
- Navidpour, S.M., Uysal, M., Kavehrad, M.: BER performance of free-space optical transmission with spatial diversity. *IEEE Trans. Wirel. Commun.* **6**, 2813–2819 (2007)
- Nossir, N., Dalil-Essakali, L., Belafhal, A.: Propagation analysis of some doughnut lasers beams through a paraxial ABCD optical system. *Opt. Quantum Electron.* **52**, 1–16 (2020a)
- Nossir, N., Dalil-Essakali, L., Belafhal, A.: Diffraction of generalized Humbert-Gaussian beams by a helical axicon. *Opt. Quantum Electron.* **53**(2), 1–13 (2021b)
- Qing, L.Y., Sen, W.Z., Jun, W.M.: Partially coherent Gaussian-Schell model pulse beam propagation in slant atmospheric turbulence. *Chin. Phys. B.* **23**(6), 064216 (2014)
- Qu, J., Zhong, Y., Zhiheng, C., Cai, Y.: Elegant Laguerre-Gaussian beam in a turbulent atmosphere. *Opt. Commun.* **283**, 2772–2781 (2010)
- Tanyer Eyyuboglu, H., Cai, Y.: Hypergeometric Gaussian beam and its propagation in turbulence. *Optics Commun.* **285**(21–22), 4194–4199 (2012)
- Wang, L.G., Zheng, W.W.: The effect of atmospheric turbulence on the propagation properties of optical vortices formed by using coherent laser beam arrays. *J. Opt. a.* **11**, 1–7 (2009)
- Wen, J.J., Breazeal, M.A., Acoustic, J.: A diffraction beam field expressed as the superposition of Gaussian beams. *Soc. Am.* **83**, 1752–1756 (1988)
- Wen, W., Chu, X., Ma, H.: The propagation of a combining Airy beam in turbulence. *Opt. Commun.* **336**, 326–329 (2015)

- Xu, J., Gao, J., Zhu, Y., Zhang, L., Zhang, Y.: Effects of atmospheric turbulence on the mode weight of the Laguerre-Gaussian Schell beams. *Optik* **125**, 280–284 (2014)
- Yaalou, M., El Halba, E.M., Hricha, Z., Belafhal, A.: Propagation characteristics of dark and antidark Gaussian beams in turbulent atmosphere. *Opt. Quantum Electron.* **51**, 2552–25510 (2019)
- Zhou, P., Liu, X., Xu, X., Chu, X.: Propagation of coherently combined flattened laser beam array in turbulent atmosphere. *Opt. Laser Technol.* **41**, 403–407 (2009)

**Publisher's Note** Springer Nature remains neutral with regard to jurisdictional claims in published maps and institutional affiliations.